

## Research

# Long noncoding RNA DDX11-AS1 represses sorafenib-induced ferroptosis in hepatocellular carcinoma cells via Nrf2-Keap1 pathway

Liang Wang<sup>1</sup> · Liming Wang<sup>1</sup>

Received: 27 October 2023 / Accepted: 7 October 2024

Published online: 10 October 2024

© The Author(s) 2024 **OPEN**

## Abstract

Sorafenib, a first-line therapeutic option for advanced hepatocellular carcinoma (HCC), faces a formidable challenge in the form of emerging resistance. Recently, the oncogene DDX11 antisense RNA 1 (DDX11-AS1) has been implicated in various cancers, including HCC. However, its role in sorafenib resistance remains unknown. Our findings reveal that DDX11-AS1 is upregulated in sorafenib-resistant HCC cells, contributing to their resistance by suppressing ferroptosis. Further investigation elucidated the mechanism by which DDX11-AS1 activates the antioxidant Nrf2-Keap1 pathway. By interacting with Nrf2 and hindering its association with Keap1, DDX11-AS1 enhances the stability and nuclear translocation of Nrf2. In summary, our study unveils the potent role of DDX11-AS1 as an enhancer of sorafenib resistance, inhibiting sorafenib-induced ferroptosis through the activation of the Nrf2-Keap1 pathway in HCC. These findings offer a promising therapeutic strategy to overcome resistance and effectively treat HCC.

**Keywords** Sorafenib · Ferroptosis · Nrf2; Keap1

## 1 Introduction

Due to the lack of surveillance and treatment options, hepatocellular carcinoma (HCC) ranks as the third most common cancer-related death worldwide, especially in developing countries [1]. During the past few decades, significant progress has been made in preventing, diagnosing, and treating HCC. However, more than half of all cases of HCC, the diagnosis is at an advanced stage, and 70% of these patients relapse within the first five years of their initial treatment [2]. Sorafenib is a first-generation targeted therapy for patients with advanced HCC who cannot undergo surgical resection. Unfortunately, due to the early occurrence of sorafenib resistance, most patients failed to experience a long-term benefit. The effectiveness of sorafenib is limited to approximately 30% of patients, and those patients usually become resistant to the drug within six months [3, 4]. Therefore, there is still a great deal of work to be done in understanding the mechanisms of sorafenib resistance in HCC patients.

Ferroptosis is a type of cell death that relies on the presence of iron and is distinct from other forms of cell death such as apoptosis, necrosis, and autophagy. The defining characteristic of ferroptosis is the buildup of harmful lipid molecules resulting from lipid peroxidation [5]. Due to the unique metabolism of cancer cells and the high load of reactive oxygen

---

**Supplementary Information** The online version contains supplementary material available at <https://doi.org/10.1007/s12672-024-01431-0>.

✉ Liang Wang, [liangsurgery@163.com](mailto:liangsurgery@163.com); ✉ Liming Wang, [wangbcc259@163.com](mailto:wangbcc259@163.com) | <sup>1</sup>The Second Affiliated Hospital of Dalian Medical University, Dalian, China, NO. 467, Zhongshan Road, Shahekou district, Liaoning 116000.



species (ROS), as well as their own specific mutations, some types of cancer cells are more susceptible to ferroptosis, thus making ferroptosis in these types as a weakness with targeted therapy potential [6]. Ferroptosis has been found to be induced by several compounds including sorafenib. The ferroptosis induced by sorafenib does not depend on its RAF kinase inhibitory effect. Sorafenib promotes ferroptosis by acting as an inhibitor of system Xc- to block SLC7A11-mediated cellular cystine import and lead to the accumulation of ROS and GSH depletion [7]. Moreover, it is likely that inhibition of ferroptosis will increase sorafenib resistance in HCC cells [8–10]. However, it is not completely understood how ferroptosis affects sorafenib resistance in HCC.

Long non-coding RNAs (lncRNAs) are a class of RNA molecules that are longer than 200 nucleotides and do not encode proteins. They have been shown to play important roles in various biological processes, including gene regulation, chromatin modification, and epigenetic regulation [11, 12]. In recent years, lncRNAs have emerged as important regulators of tumorigenesis and cancer progression. One lncRNA that has been recently studied in cancer is DDX11 antisense RNA 1 (DDX11-AS1). DDX11-AS1 is a lncRNA that is located on chromosome 10q26.13 and is transcribed in the opposite direction to the DDX11 gene. DDX11-AS1 has been shown to be dysregulated in various types of cancer, including HCC, breast cancer, lung cancer, and gastric cancer. It has been reported to play oncogenic roles in different types of cancer. DDX11-AS1 promotes cell proliferation, migration, and invasion, and induce the epithelial-mesenchymal transition (EMT), a process that is associated with cancer metastasis [13–17]. Additionally, DDX11-AS1 enhances chemoresistance in cancer cells [15, 18]. Recently, a bioinformatics analysis showed that a nine-lncRNA-based signature was identified as the ferroptosis-related prognostic model for HCC. DDX11-AS1 is one of these nine genes [19]. However, whether DDX11-AS1 acts as an anticancer hallmark for ferroptosis-mediated sorafenib resistance remains largely unknown. More research is needed to determine whether DDX11-AS1 is implicated in sorafenib resistance via ferroptosis.

In this study, we aimed to investigate the impact of DDX11-AS1 on sorafenib resistance and sorafenib-induced ferroptosis in HCC cell lines. Our findings not only shed light on a new mechanism of sorafenib resistance, but also establish a novel connection between DDX11-AS1 and ferroptosis.

## 2 Materials and methods

### 2.1 Cell culture and construction of sorafenib-resistant (SR) cells

SNU182 and Huh7 cells were obtained from the Cell Bank of the Chinese Academy of Sciences (Shanghai, China) and cultured in Dulbecco's modified Eagle's medium (DMEM) supplemented with 10% fetal bovine serum (FBS; Gibco), 100 units/mL penicillin, and 100 mg/mL streptomycin (Gibco) in a humidified incubator at 37 °C containing 5% CO<sub>2</sub>. To construct SR cells, SNU182 and Huh7 cells were first exposed to sorafenib at 5% of IC<sub>50</sub> concentration. Then, the concentration of sorafenib was gradually increased at 10% of IC<sub>50</sub> until the maximum tolerated doses was reached. To maintain the acquired resistance, SR cells (SNU182-SR and Huh7-SR) were cultured continuously in DMEM containing 1 μM concentration of sorafenib.

### 2.2 Construction of stable cell lines with overexpression or downregulation of DDX11-AS1

Recombinant lentiviruses containing full-length DDX11-AS1 or DDX11-AS1 shRNA or the control were constructed according to the standard protocol. Cells were administered with  $2 \times 10^6$  transducing units of lentiviruses and then subjected to selection with 2 μg/ml puromycin for a duration of two weeks. The target sequence of DDX11-AS1 shRNA was used as a previous study [20].

### 2.3 Cell transfection

The transfections were carried out utilizing the Lipofectamine 2000 package (Invitrogen) in accordance with the instructions provided by the manufacturer. 48 h after transfection, cells were used for further investigation.

### 2.4 Cell viability detection

Cell Counting Kit-8 (CCK-8; Dojindo) was used to assess cell viability according to the manufacturer's instructions.  $5 \times 10^3$  cells were seeded in 96-well plates with three replicate per group and treated with the corresponding concentrations

of sorafenib for 24 h. Then, 10  $\mu$ l CCK-8 reagent was added into each well and incubated for 1.5 h. The absorbance at 450 nm was assayed by microplate reader (Thermo Fisher Scientific). The half-maximal inhibitory concentration ( $IC_{50}$ ) was acquired by nonlinear regression in GraphPad Prism 9.0 software.

## 2.5 Colony formation assay

$2 \times 10^3$  cells were plated in each well of 6-well plates, with three replicates per group. The cells were cultured in DMEM supplemented with the specified drugs for a period of two weeks, with the drug-containing medium being refreshed every 72 h. After the culture period, the colonies were fixed with 4% paraformaldehyde and stained with 0.004% crystal violet. The clones were then photographed and counted.

## 2.6 Measurement of cellular iron, malondialdehyde (MDA) and glutathione (GSH)

The evaluation of lipid oxidation was evaluated by measuring the concentration of MDA in cellular lysates through the utilization of Lipid Peroxidation MDA Assay Kit (S0131, Beyotime) in accordance with the guidelines provided by the manufacturer. The levels of GSH were determined using the GSH and GSSG Assay Kit (Beyotime, S0053) following the protocol provided by the manufacturer. The intracellular  $Fe^{2+}$  concentration was quantified utilizing the Cell Ferrous Iron Colorimetric Assay Kit (Elabscience, Wuhan, China) in accordance with the manufacturer's guidelines.

## 2.7 Detection of ROS

The evaluation of lipid oxidation was evaluated using Reactive Oxygen Species (ROS) Fluorometric Assay Kit (E-BC-K138-F, Elabscience) in accordance with the manufacturer's instructions. Then, values of ROS were measured using a fluorescence microplate reader (excitation wavelength 485–515 nm, emission wavelength 510–550 nm).

## 2.8 Western blot

The proteins were separated using SDS-PAGE and then transferred to a PVDF membrane. The membranes were blocked by 10% BSA and incubated with primary antibodies at a dilution of 1:1,000 overnight. Then, the membranes were incubated with Horseradish peroxidase-conjugated antibodies to rabbit IgG or mouse IgG (each at a dilution of 1:10,000, Jackson ImmunoResearch Laboratories). The protein bands were detected using the SuperSignal West Pico Kit (Thermo Fisher) following the manufacturer's instructions. The original images of western blot were shown in Supplemental Fig. 1.

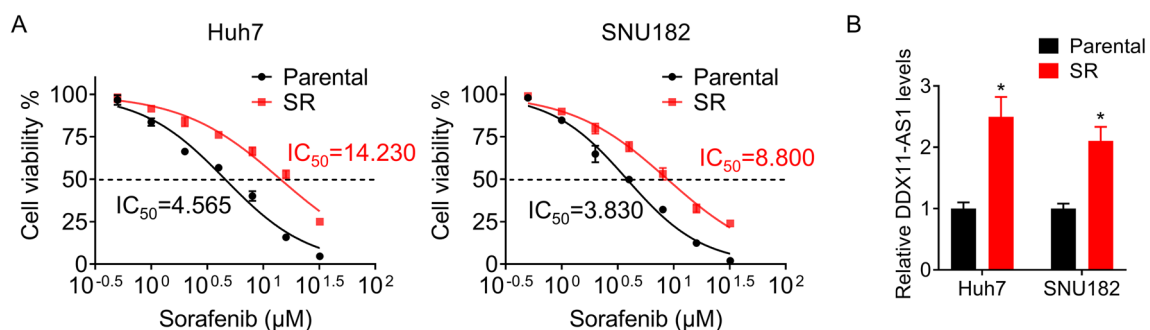


**Fig. 1** DDX11-AS1 is increased in the sorafenib-resistant HCC cells **A**. The  $IC_{50}$  values were determined for both parental and sorafenib-resistant (SR) Huh7 and SNU182 cells, which were exposed to sorafenib in a gradient concentration manner for 24 h. **B**. The expression of DDX11-AS1 in both parental and sorafenib-resistant (SR) Huh7 and SNU182 cells was tested using qRT-PCR assay.  $n = 3$  per group,  $*p < 0.05$

**Fig. 2** DDX11-AS1 induces the sorafenib resistance of HCC cells. **A.** The knockdown efficacy of DDX11-AS1 shRNA in HCC cells was tested by qRT-PCR. **B–C.** Colony formation assay of control and DDX11-AS1-silencing HCC cells treated with or without sorafenib (Sora) **D.** Cell growth curves of control and DDX11-AS1-silencing HCC cells treated with or without sorafenib was measured using CCK-8 assay. **E.** The overexpression efficacy of DDX11-AS1 in HCC cells. **F–G.** Colony formation assay of control and DDX11-AS1-overexpressing HCC cells treated with or without sorafenib. **H.** Cell growth curves of control and DDX11-AS1-overexpressing HCC cells treated with or without sorafenib was measured using CCK-8 assay. **I.** The  $IC_{50}$  values were determined for control and DDX11-AS1-silencing HCC cells, which were exposed to sorafenib in a gradient concentration manner for 24 h. **J.** The  $IC_{50}$  values were determined for control and DDX11-AS1-overexpressing HCC cells, which were exposed to sorafenib in a gradient concentration manner for 24 h n = 3 per group, \* $p < 0.05$ , \*\* $p < 0.01$ , \*\*\* $p < 0.001$

## 2.9 Isolation of nucleus and cytoplasm

The isolation of cellular nucleus and cytoplasm was performed using NE-PER™ Nuclear and Cytoplasmic Extraction Reagents (Thermo Fisher) in accordance with the manufacturer's instructions.

## 2.10 RNA isolation and quantitative real-time PCR (qRT-PCR)

The Trizol reagent (Invitrogen) was utilized to isolate the entire RNA. The M-MLV Reverse Transcriptase (Invitrogen) was employed to generate first-strand cDNA. qRT-PCR was conducted in the StepOne™ Real-Time PCR System (Applied Biosystems, Foster City, USA) with SYBR® Green (Takara, Dalian, China) and the gene-specific primers. The target RNA level was quantified based on the  $2^{-\Delta\Delta CT}$  value normalized the ACTB mRNA. Primer sequences for the genes are listed in Supplemental Table 1.

## 2.11 RNA immunoprecipitation (RIP) assay

The EZ-Magna RIP RNA Binding Protein Immunoprecipitation Kit (17–701, Millipore, USA) was utilized to conduct the RIP assay. Cells were grown until they reached 80–90% confluence, and then harvested by scraping. For each RIP reaction, 100  $\mu$ l of cell lysate from approximately  $2.0 \times 10^7$  cells was required. Subsequently, 5  $\mu$ g of purified antibodies or corresponding IgG were added to the 100- $\mu$ l cell lysate, and the mixture was rotated overnight at 4 °C. The RIP assay employed anti-Nrf2 (ab62352, Abcam), anti-Keap1 (10,503-2-AP, Proteintech) and normal rabbit IgG (PP64B, Millipore). The immunoprecipitated RNA was purified and analyzed with qRT-PCR.

## 2.12 co-immunoprecipitation (co-IP) assay

co-IP was performed by lysing cells with an IP lysis buffer (P0013, Beyotime) and incubating up to 5 mg of total protein with 50 ml of Protein G-agarose suspension (Millipore, 16–266) for 3 h at 4 °C on a rocking platform to minimize non-specific binding. The primary antibodies were added to the supernatant and incubated for an additional 3 h at 4 °C. Each immunoprecipitation mixture was then supplemented with 100 ml of Protein G-agarose and incubated overnight at 4 °C on a rocking platform. The immunoprecipitates were collected by centrifugation and washed three times with cold TBS. The agarose was boiled after adding the loading buffer and subjected to western blot assay. To prevent denaturation of heavy and light chains from antibodies used in immunoprecipitation assays, EasyBlot anti-mouse (GTX221667-01) or EasyBlot anti-rabbit (GTX221666-01) IgG HRP-conjugated secondary antibodies (Genetex) were utilized.

## 2.13 Statistical analysis

All assays were replicated independently with comparable outcomes at minimum three times. Statistical assessment and graphical representation of data were executed utilizing GraphPad Prism 9.0 software. The data were presented as mean  $\pm$  standard deviation (SD). Unless otherwise specified, distinctions between two groups were evaluated by Student's t-test, and contrasts between multiple groups were assessed by one-way analysis of variance (ANOVA) followed by Tukey's multiple comparisons test.  $p < 0.05$  was deemed statistically significant.

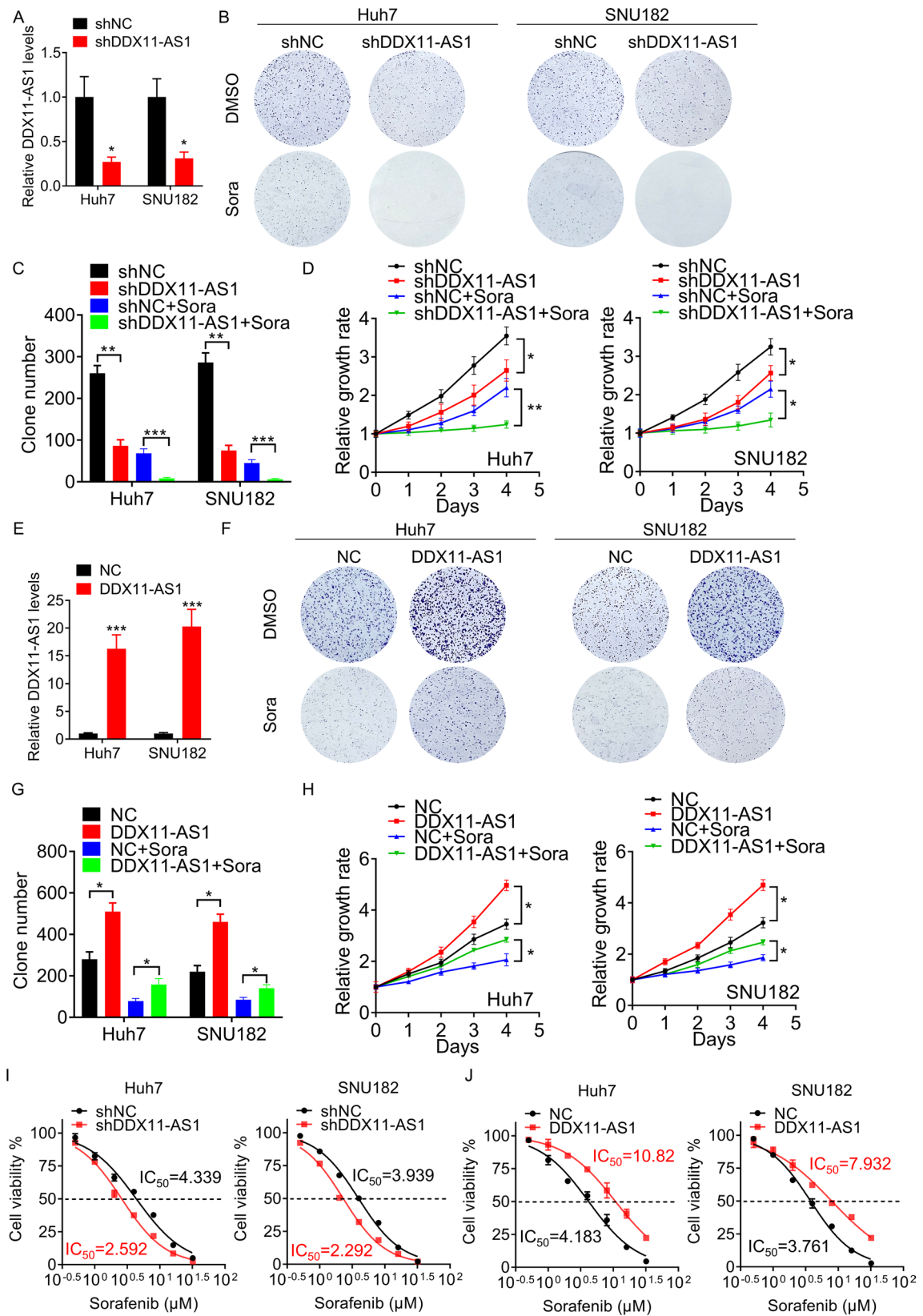


**Fig. 3** DDX11-AS1 represses sorafenib-induced ferroptosis in HCC. **A.** Control and DDX11-AS1-silencing HCC cells were treated with 10  $\mu$ M sorafenib for 24 h. Then, ROS, Fe<sup>2+</sup> and MDA levels were measured. **B.** Control and DDX11-AS1-overexpressing HCC cells were treated with 10  $\mu$ M sorafenib for 24 h. Then, ROS, Fe<sup>2+</sup> and MDA levels were measured. **C–D.** The mRNA (**C**) and protein (**D**) levels of GPX4 and SLC7A11 in control and DDX11-AS1-silencing HCC cells treated with 10  $\mu$ M sorafenib for 24 h. **E–F.** The mRNA (**E**) and protein (**F**) levels of GPX4 and SLC7A11 in control and DDX11-AS1-overexpressing HCC cells treated with 10  $\mu$ M sorafenib for 24 h. **G–H.** The mRNA (**G**) and protein (**H**) levels of GPX4 and SLC7A11 in DDX11-AS1-silencing sorafenib-resistant HCC cells treated with 10  $\mu$ M sorafenib for 24 h. **I.** Measurement of ROS, Fe<sup>2+</sup> and GSH levels in DDX11-AS1-silencing sorafenib-resistant HCC cells. **J.** DDX11-AS1-silencing sorafenib-resistant HCC cells were treated with various concentrations of sorafenib and 1  $\mu$ M Fer-1 for 24 h. The cell viability was detected using CCK-8 assay n=3 per group, \*p<0.05

## 3 Results

### 3.1 DDX11-AS1 expression is increased in sorafenib-resistant HCC cells

We conducted investigations into the molecular mechanism of sorafenib resistance in HCC by generating sorafenib-resistant (SR) HCC cell lines. This was achieved by step-wise elevating the concentration of sorafenib in the culture medium over repeated passages, resulting in the establishment of resistant Huh7 and SNU182 cell lines (named Huh7-SR and SNU182-SR). We confirmed the acquired resistance of these cells towards sorafenib by comparing them to the parental cells, with the SR cells showing 2–3 times higher half-maximal inhibitory concentrations (IC<sub>50</sub>) to sorafenib (Fig. 1A). To test whether DDX11-AS1 is involved in sorafenib resistance, we detected the differential expression of DDX11-AS1 between parental and SR cells. The qRT-PCR experiments identified a significant increase of DDX11-AS1 level in SR cell (Fig. 1B), indicating that DDX11-AS1 may facilitate sorafenib resistance in HCC cells.

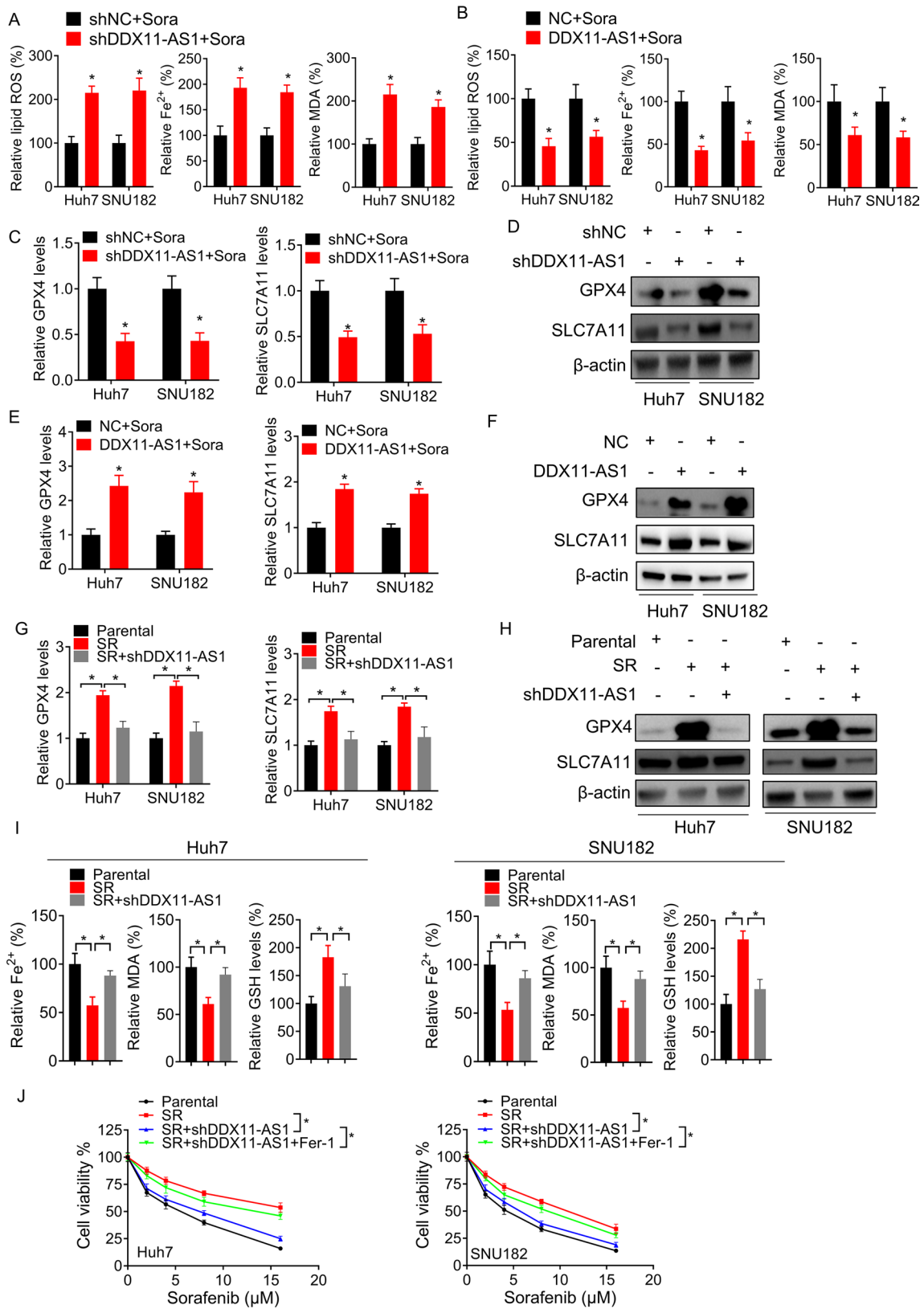
### 3.2 DDX11-AS1 promotes the resistance of HCC cells to sorafenib

Due to the upregulation of DDX11-AS1 in HCC cells resistant to sorafenib, we aimed to investigate its functional involvement in sorafenib resistance. We conducted experiments to investigate the effects of DDX11-AS1 overexpression and knockdown on the sensitivity of HCC cells to sorafenib. Firstly, a lentiviral shRNA system was utilized to knockdown DDX11-AS1 (Fig. 2A), which resulted in enhancing the sorafenib-induced growth inhibition effect as observed through colony formation and growth curves (Fig. 2B–D). Conversely, we employed the lentivirus system to overexpress DDX11-AS1 in Huh7 and SNU182 cells (Fig. 2E), which led to weakened growth inhibition effect (Fig. 2F–H). Subsequently, the cell viability of DDX11-AS1 overexpressing or silencing cells treated with sorafenib at various concentrations and time points for 24 h was analyzed using CCK-8 assays. As anticipated, DDX11-AS1 significantly attenuated the sensitivity of HCC cell lines to sorafenib. The IC<sub>50</sub> value of DDX11-AS1-silencing cells was notably lower than that of the control groups, while the IC<sub>50</sub> value was higher in cells overexpressing DDX11-AS1 (Fig. 2I–J). In summary, these findings suggest that increased DDX11-AS1 expression in HCC cells enhances their tolerance to sorafenib.

### 3.3 DDX11-AS1 represses sorafenib-induced ferroptosis in HCC

Previous studies have revealed that ferroptosis is essential for sorafenib-induced cell death in HCC [21]. In order to investigate the potential involvement of DDX11-AS1 in promoting sorafenib resistance in HCC through ferroptosis, we conducted experiments to measure levels of ROS, iron, and lipid peroxidation, which are key factors in ferroptosis, in Huh7 and SNU182 cells with DDX11-AS1 overexpression or knockdown. Our results showed that knockdown of DDX11-AS1 significantly increased levels of ROS, iron, and MDA in sorafenib-induced HCC cell lines (Fig. 3A), while induction of DDX11-AS1 decreased these levels (Fig. 3B). Additionally, we evaluated the mRNA and protein expression levels of two key genes associated with ferroptosis. DDX11-AS1 knockdown reduced the expression levels of glutathione peroxidase 4 (GPX4) and SLC7A11 in sorafenib-treated Huh7 and SNU182 cells (Fig. 3C–D). Conversely, DDX11-AS1 overexpression increased the levels of these genes (Fig. 3E–F).

Remarkably, genes linked with ferroptosis were also enhanced in Huh7-SR and SNU182-SR cells (Fig. 3G–H), which manifested relatively elevated levels of DDX11-AS1 compared to their parental cells (Fig. 1B). Simultaneously, deletion of DDX11-AS1 expression in SR cells resulted in the downregulation of ferroptosis-related genes (Fig. 3G–H), the accumulation of iron and MDA levels, and the decline of intracellular GSH level (Fig. 3I), and intensified the obstruction of sorafenib to SR cells (Fig. 3J). To further elucidate the impact of DDX11-AS1-repressed ferroptosis on sorafenib resistance,



we investigated the therapeutic effects of sorafenib by modulating the ferroptosis pathway. Our findings revealed that ferrostatin-1 (Fer-1, an inhibitor of ferroptosis) impeded the sorafenib-induced cell death in DDX11-AS1-silencing SR cells (Fig. 3J). Collectively, these findings indicated that the resistance of HCC cells to sorafenib could be augmented via the ferroptosis suppression induced by DDX11-AS1.

### 3.4 DDX11-AS1 regulates Nrf2-Keap1 pathway

The cellular defense against external and internal oxidative and electrophilic stress is primarily regulated by the nuclear factor erythroid 2-related factor (Nrf2)-Kelch-like ECH-associated protein 1 (Keap1) regulatory pathways. NRF2 is bound to KEAP1 in the cytosol, where it is directed to rapid proteasomal degradation. If stimulated, the binding of NRF2-Keap1 is unstable, Nrf2 is released, transferred to the nucleus, and binds to enhancer sequences termed “antioxidant-response elements (ARE)” to activate the transcription of downstream genes against ferroptosis, including FTH1, HO-1, NQO1, SLC7A11 and GPX4 [22–24]. Recent studies reported that the crucial function of Nrf2-Keap1 pathway activation lies in safeguarding HCC cells from ferroptosis induced by sorafenib [8, 25, 26]. To test if the Nrf2-Keap1 signaling pathway is responsible for the regulation of sorafenib-induced ferroptosis by DDX11-AS1, brusatol (an NRF2 inhibitor) or Keap1 to block the Nrf2-Keap1 pathway in cells overexpressing DDX11-AS1. Then, the levels of iron, MDA and ROS, the characteristic indicators of ferroptosis, were assessed. The findings revealed that inhibiting Nrf2-Keap1 significantly increased the accumulation of these indicators in DDX11-AS1-overexpressed cells (Fig. 4A). Conversely, using tertiary butylhydroquinone (tBHQ, an NRF2 activator) and NRF2 to activate Nrf2-Keap1 pathway produced opposite results in DDX11-AS1-silenced cells (Fig. 4B). Moreover, the qRT-PCR analysis demonstrated that the levels of target genes of Nrf2-Keap1 pathway associated with ferroptosis were altered in cells with DDX11-AS1 overexpression or knockdown upon exposure to tBHQ or brusatol (Fig. 4C–D). These findings imply that DDX11-AS1 mitigated the occurrence of ferroptosis induced by sorafenib by activating the Nrf2-Keap1 signaling pathway.

### 3.5 DDX11-AS1 associates with Nrf2

Finally, we investigated the underlying mechanism of DDX11-AS1 regulating Nrf2-Keap1 pathway. We detected the expression levels of Nrf2 and Keap1 in cells with DDX11-AS1 overexpression and knockdown. We found that DDX11-AS1 did not change their mRNA expression (Fig. 5A–B), but increased the Nrf2 protein level (Fig. 5C–D). Nrf2 is bound to Keap1, inducing its proteasomal degradation. We suspected that DDX11-AS1 may interfere the interaction between Nrf2 and Keap1. To test this, RIP assay was carried out and demonstrated that DDX11-AS1 could be enriched by Nrf2 antibody, but not by anti-Keap1 or negative control IgG antibodies (Fig. 5E). Overexpression of DDX11-AS1 dramatically attenuated the Nrf2-Keap1 interaction, whereas silence of DDX11-AS1 significantly strengthened this (Fig. 5F–G). Subsequently, the nuclear translocation of Nrf2 was examined. We isolated nuclear and cytoplasmic proteins from HCC cells with DDX11-AS1 alteration. As anticipated, cells overexpressing DDX11-AS1 exhibited an elevated enrichment of Nrf2 in the cell nucleus, while knockdown of DDX11-AS1 resulted in the cytoplasmic translocation of Nrf2 (Fig. 5H–I). Based on this, we verified that DDX11-AS1 has the capability to prompt the movement of Nrf2 to the nucleus through direct interaction.

## 4 Discussion

The global incidence of HCC continues to rise, with high rates of both occurrence and mortality [1]. Overcoming resistance to the drug sorafenib remains a significant challenge in HCC treatment, greatly impacting patient prognosis [3, 4]. Therefore, in order to improve the efficacy of chemotherapy and guide clinical medication, it is crucial to fully understand the mechanisms underlying sorafenib resistance in HCC. In this study, we discovered that upregulation of DDX11-AS1 induced the activation of the Nrf2-Keap1 pathway, leading to inhibition of sorafenib-induced cell death. This was accompanied by a decrease in iron accumulation, lipid peroxidation, and subsequent ferroptosis. Thus, targeting the DDX11-AS1 or Nrf2-Keap1 pathway to enhance the anticancer effects of sorafenib through induction of ferroptosis holds great promise as a therapeutic strategy for HCC treatment.

The precise mechanism through which DDX11-AS1 exerts its regulatory influence on gene expression and cellular processes in cancer remains incompletely elucidated. Several investigations have proposed that DDX11-AS1 may operate as a competing endogenous RNA (ceRNA), effectively sequestering microRNAs and modulating the expression of their target genes. For instance, in HCC, DDX11-AS1 has been demonstrated to act as a miR-34a or miR1-9 sponge, thereby

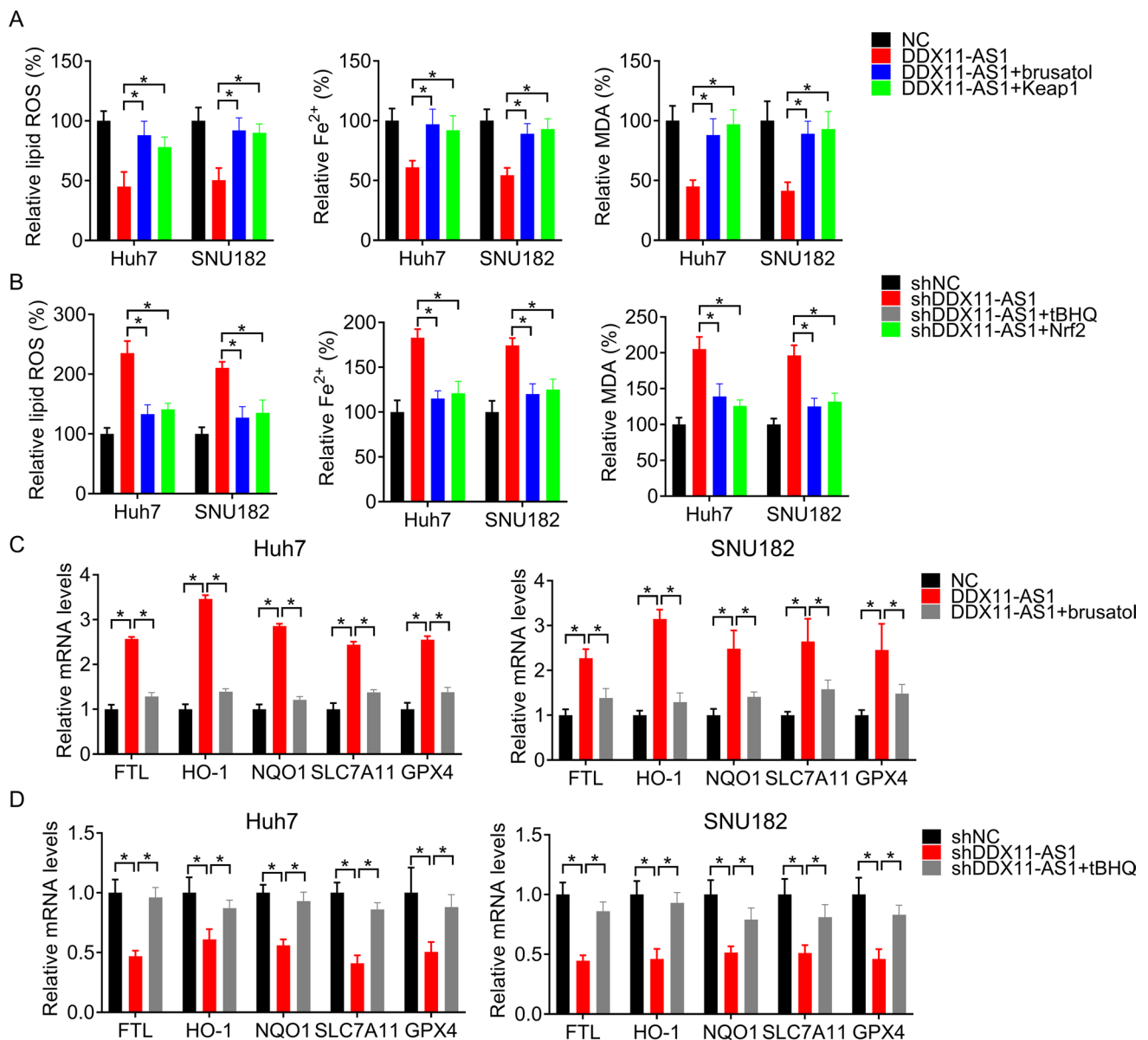


**Fig. 4** DDX11-AS1 regulates Nrf2-Keap1 pathway. **A.** Measurement of cellular ROS, iron and MDA levels in DDX11-AS1-overexpressing HCC cells treated with sorafenib (10  $\mu$ M for 24 h) alone or co-treatment with brusatol (40 nM for 12 h) or transfected with Keap1. **B.** Measurement of cellular ROS, iron and MDA levels in DDX11-AS1-knockdown HCC cells treated with sorafenib (10  $\mu$ M for 24 h) alone or co-treatment with tBHQ (100  $\mu$ M for 6 h) or transfected with Nrf2. **C.** qRT-PCR analysis of the mRNA expression levels of indicated genes in DDX11-AS1-overexpressing HCC cells treated with sorafenib (10  $\mu$ M for 24 h) alone or co-treatment with brusatol (40 nM for 12 h). **D.** qRT-PCR analysis of the mRNA expression levels of indicated genes in DDX11-AS1-knockdown HCC cells treated with sorafenib (10  $\mu$ M for 24 h) alone or co-treatment with tBHQ (100  $\mu$ M for 6 h). n=3 per group, \*p<0.05

modulating the expression of its downstream target, TRAF5 or MACC1 [13, 27]. Similarly, in esophageal squamous cell carcinoma, DDX11-AS1 has been observed to function as a miR-30d sponge, thereby regulating the expression of SNAI1/ZEB2 and inducing epithelial mesenchymal transition [28]. Additionally, DDX11-AS1 may also exert its impact on the development of chemoresistance by modulating the intricate machinery of DNA damage repair or regulating the ATG7 and ATG 12 expression [15, 18]. Here, we elucidated a novel functional role of DDX11-AS1 in HCC. Our in vitro experiments demonstrated that DDX11-AS1 inhibited the sorafenib-induced ferroptosis, enhancing the resistance of HCC cells to sorafenib treatment. Further in vivo experiments will provide even stronger support for our findings.

Ferroptosis primarily arises from the impairment of the cellular antioxidant system, particularly the system Xc<sup>-</sup>-glutathione (GSH)-GPX4-dependent defense mechanism. This impairment results in the accumulation of lipid

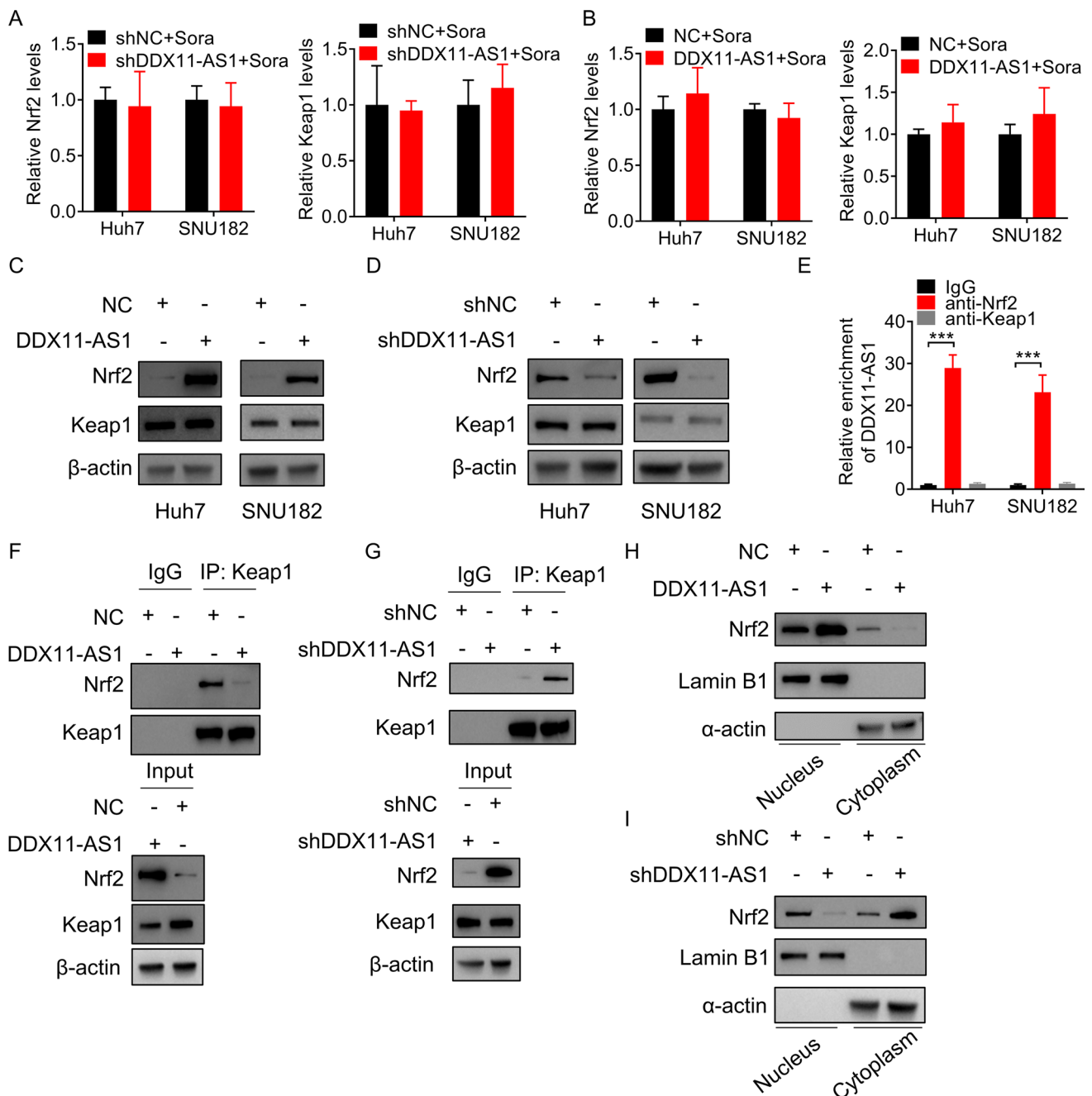


**Fig. 5** DDX11-AS1 associates with Nrf2. **A–B.** The mRNA levels of Nrf2 and Keap1 were measured using qRT-PCR assays in control and DDX11-AS1-silencing (**A**) or -overexpressing (**B**) HCC cells treated with 10 μM sorafenib for 24 h. **C–D.** The protein levels of Nrf2 and Keap1 was measured using western blot assay in control and DDX11-AS1-overexpressing (**C**) or -silencing (**D**) HCC cells treated with 10 μM sorafenib for 24 h. **E.** The RIP assay followed by qRT-PCR was conducted using negative control IgG, anti-Nrf2 or anti-Keap1 antibodies in HCC cells treated with 10 μM sorafenib for 24 h. **F–G.** co-IP experiments using IgG or anti-Keap1 antibodies were performed in control and DDX11-AS1 overexpressed (**F**) or knockdown (**G**) Huh7 cells treated with 10 μM sorafenib for 24 h. **H–I.** The nuclear and cytoplasmic Nrf2 was examined using western blot assay in control and DDX11-AS1 overexpressed (**H**) or knockdown (**I**) Huh7 cells treated with 10 μM sorafenib for 24 h. Lamin B1 and α-actin was used as nuclear and cytoplasmic internal reference, respectively. n = 3 per group, \*\*\*p < 0.001

hydroperoxides. The system Xc – antiporter is accountable for the transmembrane uptake of extracellular cystine, which is subsequently converted to intracellular cysteine, a crucial precursor for GSH synthesis. GSH serves as an essential coenzyme for the proper functioning of GPX4, an antioxidant enzyme that effectively neutralizes phospholipid hydroperoxide. As a cystine and glutamate antiporter, system Xc- in the plasma membrane is a heterodimeric protein complex comprised of SLC7A11 and solute carrier family 3 member 2 (SLC3A2) [29]. The genes

GPX4 and SLC7A11 have been identified as well-established transcriptional targets of the transcription factor Nrf2, which exerts transcriptional regulation over a significant portion of genes associated with ferroptosis. Activation of Nrf2-Keap1-GPX4/SLC7A11 pathway was found to be closely associated with cancer progression via ferroptosis [30–32]. In this study, we have uncovered a novel regulatory mechanism of the Nrf2-Keap1 signaling pathway mediated by DDX11-AS1. DDX11-AS1 forms an intricate association with Nrf2, shielding it from the clutches of Keap1 and preventing its degradation, thereby facilitating its translocation into the nucleus. We postulate that DDX11-AS1 may occupy a crucial domain within Nrf2 that is responsible for its interaction with Keap1. Moreover, DDX11-AS1 increased the expression of GPX4 and SLC7A11, which could be reversed by inhibition of Nrf2-Keap1 signaling.

## 5 Conclusion

Our investigation reveals the impact of DDX11-AS1 as a catalyst for sorafenib resistance, impeding sorafenib-triggered ferroptosis by activating the Nrf2-Keap1 pathway in HCC. These discoveries present an auspicious therapeutic approach to surmount resistance and efficaciously manage HCC.

**Acknowledgements** Not applicable.

**Author contributions** The research was meticulously crafted by all the authors, who conducted experiments and meticulously scrutinized the data. Liang Wang and Liming Wang took charge of writing the manuscript. The final manuscript was thoroughly reviewed and endorsed by all authors. The datasets generated during the current study are available from the corresponding author on reasonable request.

**Funding** None.

**Data availability** The datasets generated during the current study are available from the corresponding author on reasonable request.

## Declarations

**Ethics approval and consent to participate** The present study was approved by the Ethics Committee of the First Affiliated Hospital of Jinzhou Medical University and carried out in accordance with the World Medical Association Declaration of Helsinki.

**Consent for publication** Not applicable.

**Competing interests** The authors declare no competing interests.

**Open Access** This article is licensed under a Creative Commons Attribution-NonCommercial-NoDerivatives 4.0 International License, which permits any non-commercial use, sharing, distribution and reproduction in any medium or format, as long as you give appropriate credit to the original author(s) and the source, provide a link to the Creative Commons licence, and indicate if you modified the licensed material. You do not have permission under this licence to share adapted material derived from this article or parts of it. The images or other third party material in this article are included in the article's Creative Commons licence, unless indicated otherwise in a credit line to the material. If material is not included in the article's Creative Commons licence and your intended use is not permitted by statutory regulation or exceeds the permitted use, you will need to obtain permission directly from the copyright holder. To view a copy of this licence, visit <http://creativecommons.org/licenses/by-nc-nd/4.0/>.

## References

1. Sung H, Ferlay J, Siegel RL, Laversanne M, Soerjomataram I, Jemal A, et al. Global cancer statistics 2020: GLOBOCAN estimates of incidence and mortality worldwide for 36 cancers in 185 countries. *CA Cancer J Clin*. 2021;71(3):209–49. <https://doi.org/10.3322/caac.21660>.
2. Llovet JM, Zucman-Rossi J, Pikarsky E, Sangro B, Schwartz M, Sherman M, et al. Hepatocellular carcinoma. *Nat Rev Dis Primers*. 2016;2:16018. <https://doi.org/10.1038/nrdp.2016.18>.
3. Guo L, Hu C, Yao M, Han G. Mechanism of sorafenib resistance associated with ferroptosis in HCC. *Front Pharmacol*. 2023;14:1207496. <https://doi.org/10.3389/fphar.2023.1207496>.
4. Girardi DM, Sousa LP, Miranda TA, Haum FNC, Pereira GCB, Pereira AAL. Systemic therapy for advanced hepatocellular carcinoma: current stand and perspectives. *Cancers*. 2023. <https://doi.org/10.3390/cancers15061680>.
5. Dos Santos AF, Fazeli G, Xavier da Silva TN, Friedmann Angeli JP. Ferroptosis mechanisms and implications for cancer development and therapy response. *Trends Cell Biol*. 2023. <https://doi.org/10.1016/j.tcb.2023.04.005>.
6. Liu Y, Wang P, Hu W, Chen D. New insights into the roles of peroxiredoxins in cancer. *Biomed Pharmacother*. 2023;164: 114896. <https://doi.org/10.1016/j.biopha.2023.114896>.

7. Dixon SJ, Patel DN, Welsch M, Skouta R, Lee ED, Hayano M, et al. Pharmacological inhibition of cystine-glutamate exchange induces endoplasmic reticulum stress and ferroptosis. *Elife*. 2014;3: e02523. <https://doi.org/10.7554/eLife.02523>.
8. Xu FL, Wu XH, Chen C, Wang K, Huang LY, Xia J, et al. SLC27A5 promotes sorafenib-induced ferroptosis in hepatocellular carcinoma by downregulating glutathione reductase. *Cell Death Dis*. 2023;14(1):22. <https://doi.org/10.1038/s41419-023-05558-w>.
9. Liu L, Lv Z, Wang M, Zhang D, Liu D, Zhu F. HBV enhances sorafenib resistance in hepatocellular carcinoma by reducing ferroptosis via SRSF2-mediated abnormal PCLAF splicing. *Int J Mol Sci*. 2023. <https://doi.org/10.3390/ijms24043263>.
10. Li X, Li Y, Lian P, Lv Q, Liu F. Silencing lncRNA HCG18 regulates GPX4-inhibited ferroptosis by adsorbing miR-450b-5p to avert sorafenib resistance in hepatocellular carcinoma. *Hum Exp Toxicol*. 2023;42:9603271221142818. <https://doi.org/10.1177/09603271221142818>.
11. Verma S, Sahu BD, Mugale MN. Role of lncRNAs in hepatocellular carcinoma. *Life Sci*. 2023;325: 121751. <https://doi.org/10.1016/j.lfs.2023.121751>.
12. Ge WJ, Huang H, Wang T, Zeng WH, Guo M, Ren CR, et al. Long non-coding RNAs in hepatocellular carcinoma. *Pathol Res Pract*. 2023;248: 154604. <https://doi.org/10.1016/j.prp.2023.154604>.
13. Wan T, Zheng J, Yao R, Yang S, Zheng W, Zhou P. lncRNA DDX11-AS1 accelerates hepatocellular carcinoma progression via the miR-195-5p/MACC1 pathway. *Ann Hepatol*. 2021;20: 100258. <https://doi.org/10.1016/j.aohp.2020.09.003>.
14. Song W, Qian Y, Zhang MH, Wang H, Wen X, Yang XZ, et al. The long non-coding RNA DDX11-AS1 facilitates cell progression and oxaliplatin resistance via regulating miR-326/IRS1 axis in gastric cancer. *Eur Rev Med Pharmacol Sci*. 2020;24(6):3049–61. [https://doi.org/10.26355/eurrev\\_202003\\_20669](https://doi.org/10.26355/eurrev_202003_20669).
15. Si X, Zhang G, Li M, Yao M, Shi X, Dong Z, et al. lncRNA DDX11-AS1 Promotes Chemoresistance through LIN28A-Mediated ATG12 mRNA Stabilization in Breast Cancer. *Pharmacology*. 2023;108(1):61–73. <https://doi.org/10.1159/000527222>.
16. Ren Z, Liu X, Si Y, Yang D. Long non-coding RNA DDX11-AS1 facilitates gastric cancer progression by regulating miR-873-5p/SPC18 axis. *Artif Cells Nanomed Biotechnol*. 2020;48(1):572–83. <https://doi.org/10.1080/21691401.2020.1726937>.
17. Li Y, Zhuang W, Huang M, Li X. Long noncoding RNA DDX11-AS1 epigenetically represses LATS2 by interacting with EZH2 and DNMT1 in hepatocellular carcinoma. *Biochem Biophys Res Commun*. 2019;514(4):1051–7. <https://doi.org/10.1016/j.bbrc.2019.05.042>.
18. Liu J, Yang X, Gao S, Wen M, Yu Q. DDX11-AS1 modulates DNA damage repair to enhance paclitaxel resistance of lung adenocarcinoma cells. *Pharmacogenomics*. 2023;24(3):163–72. <https://doi.org/10.2217/pgs-2022-0121>.
19. Xu Z, Peng B, Liang Q, Chen X, Cai Y, Zeng S, et al. Construction of a ferroptosis-related nine-lncRNA signature for predicting prognosis and immune response in hepatocellular carcinoma. *Front Immunol*. 2021;12: 719175. <https://doi.org/10.3389/fimmu.2021.719175>.
20. Xu M, Zhao X, Zhao S, Yang Z, Yuan W, Han H, et al. Landscape analysis of lncRNAs shows that DDX11-AS1 promotes cell-cycle progression in liver cancer through the PARP1/p53 axis. *Cancer Lett*. 2021;520:282–94. <https://doi.org/10.1016/j.canlet.2021.08.001>.
21. Zhang L, Li XM, Shi XH, Ye K, Fu XL, Wang X, et al. Sorafenib triggers ferroptosis via inhibition of HBXIP/SCD axis in hepatocellular carcinoma. *Acta Pharmacol Sin*. 2023;44(3):622–34. <https://doi.org/10.1038/s41401-022-00981-9>.
22. Yan R, Lin B, Jin W, Tang L, Hu S, Cai R. NRF2, a superstar of ferroptosis. *Antioxidants*. 2023. <https://doi.org/10.3390/antiox12091739>.
23. Toyokuni S, Ito F, Yamashita K, Okazaki Y, Akatsuka S. Iron and thiol redox signaling in cancer: an exquisite balance to escape ferroptosis. *Free Radic Biol Med*. 2017;108:610–26. <https://doi.org/10.1016/j.freeradbiomed.2017.04.024>.
24. Lee J, Roh JL. Targeting Nrf2 for ferroptosis-based therapy: Implications for overcoming ferroptosis evasion and therapy resistance in cancer. *Biochim Biophys Acta Mol Basis Dis*. 2023;1869(7): 166788. <https://doi.org/10.1016/j.bbadis.2023.166788>.
25. Wang Q, Bin C, Xue Q, Gao Q, Huang A, Wang K, et al. GSTZ1 sensitizes hepatocellular carcinoma cells to sorafenib-induced ferroptosis via inhibition of NRF2/GPX4 axis. *Cell Death Dis*. 2021;12(5):426. <https://doi.org/10.1038/s41419-021-03718-4>.
26. Houesson A, Francois C, Sauzay C, Louandre C, Mongelard G, Godin C, et al. Metallothionein-1 as a biomarker of altered redox metabolism in hepatocellular carcinoma cells exposed to sorafenib. *Mol Cancer*. 2016;15(1):38. <https://doi.org/10.1186/s12943-016-0526-2>.
27. Ding G, Zeng Y, Yang D, Zhang C, Mao C, Xiao E, et al. Silenced lncRNA DDX11-AS1 or up-regulated microRNA-34a-3p inhibits malignant phenotypes of hepatocellular carcinoma cells via suppression of TRAF5. *Cancer Cell Int*. 2021;21(1):179. <https://doi.org/10.1186/s12935-021-01847-6>.
28. Guo Y, Sun P, Guo W, Yin Q, Han J, Sheng S, et al. lncRNA DDX11 antisense RNA 1 promotes EMT process of esophageal squamous cell carcinoma by sponging miR-30d-5p to regulate SNAI1/ZEB2 expression and Wnt/beta-catenin pathway. *Bioengineered*. 2021;12(2):11425–40. <https://doi.org/10.1080/21655979.2021.2008759>.
29. Chen X, Li J, Kang R, Klionsky DJ, Tang D. Ferroptosis: machinery and regulation. *Autophagy*. 2021;17(9):2054–81. <https://doi.org/10.1080/15548627.2020.1810918>.
30. Shi J, Ma C, Zheng Z, Zhang T, Li Z, Sun X, et al. Low-dose antimony exposure promotes prostate cancer proliferation by inhibiting ferroptosis via activation of the Nrf2-SLC7A11-GPX4 pathway. *Chemosphere*. 2023;339: 139716. <https://doi.org/10.1016/j.chemosphere.2023.139716>.
31. Liu X, Yan C, Chang C, Meng F, Shen W, Wang S, et al. FOXA2 suppression by TRIM36 exerts anti-tumor role in colorectal cancer via inducing NRF2/GPX4-regulated ferroptosis. *Adv Sci*. 2023. <https://doi.org/10.1002/advs.202304521>.
32. Rosell R, Jain A, Codony-Servat J, Jantus-Lewintre E, Morrison B, Ginesta JB, et al. Biological insights in non-small cell lung cancer. *Cancer Biol Med*. 2023;20(7):500–18. <https://doi.org/10.20892/j.issn.2095-3941.2023.0108>.

**Publisher's Note** Springer Nature remains neutral with regard to jurisdictional claims in published maps and institutional affiliations.